Vol 12 No 9, September 2003
1009-1963/2003/12(09)/1001-06
Chinese Physics
© 2003 Chin. Phys. Soc.
and IOP Publishing Ltd

Study of the behaviour of the fibre Bragg grating fabricated with cladding mode suppression fibre*

Xu Xin-Hua(徐新华), Lü Chang-Gui(吕昌贵), and Cui Yi-Ping(崔一平)†

Department of Electronic Engineering, Southeast University, Nanjing 210096, *China*

(Received 7 March 2003; revised manuscript received 31 March 2003)

One effective method for suppression of coupling from guided optical modes into cladding modes in an optical fibre Bragg grating is to use cladding mode suppression fibre. In this specially engineered fibre, the grating is written into the core and the inner cladding, both of which are photosensitive. A theory is presented in this paper to analyse the spectral characteristics of this kind of gratings. A fibre Bragg grating was experimentally fabricated with this kind of photosensitive fibre (PS-RMS-50 from StockerYale). It is shown both theoretically and experimentally that such gratings exhibit strong suppression of the coupling between core mode and cladding mode. The experimental result is in good agreement with the theoretical analysis.

Keywords: coupled mode analysis, gratings, wavelength division multiplexing (WDM)
PACC: 4281W, 4281, 4280S, 4280

1. Introduction

In recent years, extensive and in-depth studies have been performed covering various kinds of fibre gratings including fibre Bragg gratings[1−3] and long-period fibre gratings.[4,5] Up to now, much progress has been made. In this research, fibre Bragg gratings attract great attention due to its important applications in wavelength division multiplexing (WDM) systems. However, in a fibre grating with a photosensitive core, the forward-propagating guided core mode (LP_{01}) does not only couple with the backward-propagating guided core mode itself but also couple with the backward-propagating cladding modes. These couplings generate a series of loss peaks in the transmission spectrum at wavelengths below the main reflection peak. These loss peaks restrict the use of these gratings in WDM systems. In 1995, Delevaque *et al* designed and fabricated a fibre with a photosensitive inner cladding between the core and the outer cladding.[6] By using this kind of fibre, they successfully imprinted a highly reflective Bragg grating with a strong reduction of extra losses due to cladding mode coupling. An experiment and a brief explanation were given by them. In this paper, we consider the details of the suppression of coupling from guided mode into cladding modes for the Bragg gratings fabricated with the cladding mode suppression fibre. Both theory for understanding the principle and methods of calculation are presented. Furthermore, we use the cladding mode suppression fibre (PS-RMS-50) to write a Bragg grating and then compare the experimentally measured transmission spectrum with the calculations based on the theory.

2. Theory

2.1. Modes and fields

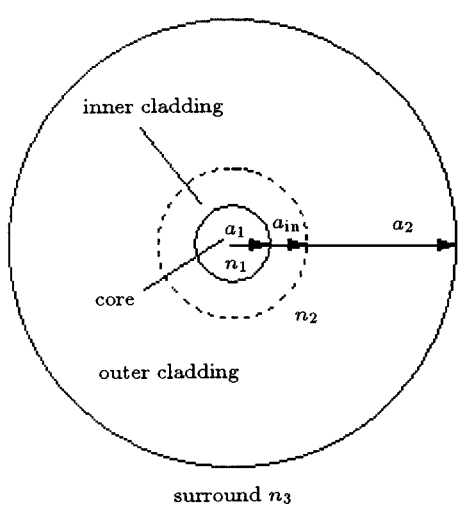


Fig.1. Diagram of a cross section of the cladding mode suppression fibre.

*Project supported by the National Science Foundation of China for Distinguished Young Scholars (Grant No 60125513).
†Corresponding author. E-mail: ypcyz@seu.edu.cn

Figure 1 shows the cross section of the cladding mode suppression fibre (PS-RMS-50). The fibre consists of a core of radius a_1, with refractive index n_1, an inner cladding of radius $a_{\rm in}$, and an outer cladding of radius a_2. The inner and the outer claddings have the same refractive index n_2, with the difference that the inner cladding has the same photosensitivity as the core. So when we analyse the modes and fields in the fibre, we can still use the simple three-layer-model which assumes that the fibre consists of a core of radius a_1, with refractive index n_1, and a cladding of radius a_2, with refractive index n_2, surrounded by an infinite uniform medium of refractive index n_3.

Because the optical fibre Bragg gratings considered in this paper has a circularly symmetric perturbation, the coupling is limited to cladding modes with azimuthal order 1. Therefore, here we just list the fields and the dispersion relations of the core mode ($\rm LP_{01}$ or $\rm HE_{11}$) and the cladding modes $\rm HE_{1\nu}$.

The radial and azimuthal vector components of the $\rm HE_{11}$ mode fields are given by

$$E_r^{\rm co}=\begin{cases}{\rm i}E_{01}^{\rm co}\dfrac{{\rm J}_0(ur/a_1)}{{\rm J}_0(u)}\exp({\rm i}\phi)\exp[{\rm i}(\beta z-\omega t)] & (r\le a_1),\\ {\rm i}E_{01}^{\rm co}\dfrac{{\rm K}_0(wr/a_1)}{{\rm K}_0(w)}\exp({\rm i}\phi)\exp[{\rm i}(\beta z-\omega t)] & (r>a_1),\end{cases}\tag{1}$$

$$E_\phi^{\rm co}=\begin{cases}-E_{01}^{\rm co}\dfrac{{\rm J}_0(ur/a_1)}{{\rm J}_0(u)}\exp({\rm i}\phi)\exp[{\rm i}(\beta z-\omega t)] & (r\le a_1),\\ -E_{01}^{\rm co}\dfrac{{\rm K}_0(wr/a_1)}{{\rm K}_0(w)}\exp({\rm i}\phi)\exp[{\rm i}(\beta z-\omega t)] & (r>a_1),\end{cases}\tag{2}$$

where J is a Bessel function of the first kind, K is a modified Bessel function of the second kind, β is the propagation constant, given by $\beta=(2\pi/\lambda)n_{\rm eff}^{\rm co}$, and $u=a_1(k_0^2n_1^2-\beta^2)^{1/2}$, $w=a_1(\beta^2-k_0^2n_2^2)^{1/2}$, and $E_{01}^{\rm co}$ is the normalization constant, based on a total power of 1 W carried by the mode, which is given by

$$\begin{aligned}E_{01}^{\rm co}=&\frac{u}{V}\frac{{\rm K}_0(w)}{{\rm K}_1(w)}\left[\frac{2Z_0}{\pi a_1^2n_2}\right]^{1/2}\\ =&\frac{w}{V}\frac{{\rm J}_0(u)}{{\rm J}_1(u)}\left[\frac{2Z_0}{\pi a_1^2n_2}\right]^{1/2},\end{aligned}\tag{3}$$

where $Z_0=\sqrt{\mu_0/\varepsilon_0}=377\Omega$ is the electromagnetic impedance in vacuum. The z-axis is along the axis of the fibre, $V=a_1(k_0^2n_1^2-k_0^2n_2^2)^{1/2}$ is the V number of the fibre at a wavelength λ, $k_0=2\pi/\lambda$ is the wavenumber in vacuum.

The radial and azimuthal vector components of the electric field for the cladding mode $\rm HE_{1\nu}$ in the fibre core ($r\le a_1$) are given by[7]

$$\begin{aligned}E_r^{\rm cl}=&{\rm i}E_{1\nu}^{\rm cl}\frac{u_1}{2}\Big\{{\rm J}_2(u_1r)+{\rm J}_0(u_1r)\\ &-\frac{\sigma_2\xi_0}{n_1^2}[{\rm J}_2(u_1r)-{\rm J}_0(u_1r)]\Big\}\\ &\times\exp({\rm i}\phi)\exp[{\rm i}(\beta z-\omega t)]\quad(r\le a_1),\end{aligned}\tag{4}$$

and

$$\begin{aligned}E_\phi^{\rm cl}=&E_{1\nu}^{\rm cl}\frac{u_1}{2}\Big\{{\rm J}_2(u_1r)-{\rm J}_0(u_1r)\\ &-\frac{\sigma_2\xi_0}{n_1^2}[{\rm J}_2(u_1r)+{\rm J}_0(u_1r)]\Big\}\\ &\times\exp({\rm i}\phi)\exp[{\rm i}(\beta z-\omega t)]\quad(r\le a_1),\end{aligned}\tag{5}$$

where ν is the cladding-mode number and $E_{1\nu}^{\rm cl}$ is the field normalization constant, which is calculated by assuming the cladding mode $\rm HE_{1\nu}^{cl}$ carries a power of 1W.

The radial and azimuthal vector components of the electric field for the cladding mode $\rm HE_{1\nu}$ in the fibre cladding region ($a_1\le r\le a_2$) are given by[7]

$$\begin{aligned}E_r^{\rm cl}=&{\rm i}E_{1\nu}^{\rm cl}\frac{\pi a_1u_1^2{\rm J}_1(u_1a_1)}{2}\Big\{-\frac{F_2}{r}p_1(r)+\frac{1}{u_2r}q_1(r)\\ &-\frac{\sigma_2}{n_2^2}\left[u_2G_2r_1(r)-\frac{n_2^2\xi_0}{n_1^2}s_1(r)\right]\Big\}\\ &\times\exp({\rm i}\phi)\exp[{\rm i}(\beta z-\omega t)]\quad(a_1\le r\le a_2),\end{aligned}\tag{6}$$

and

$$\begin{aligned}E_\phi^{\rm cl}=&E_{1\nu}^{\rm cl}\frac{\pi a_1u_1^2{\rm J}_1(u_1a_1)}{2}\Big\{\frac{\sigma_2}{n_2^2}\left[\frac{G_2}{r}p_1(r)\right.\\ &\left.-\frac{n_2^2\xi_0}{n_1^2u_2r}q_1(r)\right]+u_2F_2r_1(r)-s_1(r)\Big\}\\ &\times\exp({\rm i}\phi)\exp[{\rm i}(\beta z-\omega t)]\quad(a_1\le r\le a_2).\end{aligned}\tag{7}$$

The following definitions have been used Eqs.(4)–(7)

$$\zeta_0 = \frac{1}{\sigma_2}\frac{u_2\left(\mathrm{JK} + \dfrac{\sigma_1\sigma_2 u_{21}u_{32}}{n_2^2 a_1 a_2}\right)p_1(a_2) - \mathrm{K}q_1(a_2) + \mathrm{J}r_1(a_2) - \dfrac{1}{u_2}s_1(a_2)}{-u_2\left(\dfrac{u_{32}}{n_2^2 a_2}\mathrm{J} - \dfrac{u_{21}}{n_1^2 a_1}\mathrm{K}\right)p_1(a_2) + \dfrac{u_{32}}{n_1^2 a_2}q_1(a_2) + \dfrac{u_{21}}{n_1^2 a_1}r_1(a_2)}, \tag{8}$$

$$F_2 \equiv \mathrm{J} - \frac{u_{21}\sigma_2\xi_0}{n_1^2 a_1}, \tag{9}$$

$$G_2 \equiv \xi_0\mathrm{J} + \frac{u_{21}\sigma_1}{a_1}, \tag{10}$$

$$\sigma_1 = \mathrm{i}n_{\mathrm{eff}}^{\mathrm{cl}}/Z_0, \tag{11}$$

$$\sigma_2 = \mathrm{i}n_{\mathrm{eff}}^{\mathrm{cl}}Z_0, \tag{12}$$

$$u_{21} = \frac{1}{u_2^2} - \frac{1}{u_1^2}, \tag{13}$$

$$u_{32} = \frac{1}{w_3^2} + \frac{1}{u_2^2}, \tag{14}$$

$$u_j^2 = (2\pi/\lambda)^2(n_j^2 - (n_{\mathrm{eff}}^{\mathrm{cl}})^2), \quad j = 1, 2, \tag{15}$$

$$w_3^2 = (2\pi/\lambda)^2((n_{\mathrm{eff}}^{\mathrm{cl}})^2 - n_3^2), \tag{16}$$

$$\mathrm{J} = \frac{\mathrm{J}_1'(u_1a_1)}{u_1\mathrm{J}_1(u_1a_1)}, \tag{17}$$

$$\mathrm{K} = \frac{\mathrm{K}_1'(w_3a_2)}{w_3\mathrm{K}_1(w_3a_2)}, \tag{18}$$

$$p_1(r) = \mathrm{J}_1(u_2r)\mathrm{N}_1(u_2a_1) - \mathrm{J}_1(u_2a_1)\mathrm{N}_1(u_2r), \tag{19}$$

$$q_1(r) = \mathrm{J}_1(u_2r)\mathrm{N}_1'(u_2a_1) - \mathrm{J}_1'(u_2a_1)\mathrm{N}_1(u_2r), \tag{20}$$

$$r_1(r) = \mathrm{J}_1'(u_2r)\mathrm{N}_1(u_2a_1) - \mathrm{J}_1(u_2a_1)\mathrm{N}_1'(u_2r), \tag{21}$$

$$s_1(r) = \mathrm{J}_1'(u_2r)\mathrm{N}_1'(u_2a_1) - \mathrm{J}_1'(u_2a_1)\mathrm{N}_1'(u_2r). \tag{22}$$

The dispersion relation that we solve to obtain the LP_{01} mode effective index is

$$u\frac{\mathrm{J}_1(u)}{\mathrm{J}_0(u)} = w\frac{\mathrm{K}_1(w)}{\mathrm{K}_0(w)}. \tag{23}$$

The dispersion relation of the cladding mode $\mathrm{HE}_{1\nu}$ is[7]

$$\xi_0 = \xi_0', \tag{24}$$

$$\zeta_0' = -\sigma_1\frac{u_2\left(\dfrac{u_{32}}{a_2}\mathrm{J} - \dfrac{n_3^2u_{21}}{n_2^2a_1}\mathrm{K}\right)p_1(a_2) + \dfrac{u_{32}}{a_2}q_1(a_2) + \dfrac{u_{21}}{a_1}r_1(a_2)}{u_2\left(\dfrac{n_3^2}{n_2^2}\mathrm{JK} + \dfrac{\sigma_1\sigma_2u_{21}u_{32}}{n_1^2a_1a_2}\right)p_1(a_2) - \dfrac{n_3^2}{n_1^2}\mathrm{K}q_1(a_2) + \mathrm{J}r_1(a_2) - \dfrac{n_2^2}{n_1^2u_2}s_1(a_2)}. \tag{25}$$

2.2. Coupling coefficients

In this section we calculate the coupling coefficients for coupling between the LP_{01} core mode and itself and between the LP_{01} core mode and the $\mathrm{HE}_{1\nu}^{\mathrm{cl}}$ cladding mode, respectively.

Because both the core and the inner cladding are photosensitive, when a phase grating is induced in the fibre, it exists not only in the core but also in the inner cladding. As a result, the core index is changed to $n_1(z)$, the inner cladding index is changed to $n_2(z)$ and the outer cladding and surround indices are unchanged:

$$n(r,z) = \begin{cases} n_1(z) = n_1 + \overline{\delta n}(z)[1 + m\cos(2\pi z/\Lambda)], & r \le a_1, \\ n_2(z) = n_2 + \overline{\delta n}(z)[1 + m\cos(2\pi z/\Lambda)], & a_1 < r \le a_{\mathrm{in}}, \\ n_2, & a_{\mathrm{in}} < r \le a_2, \\ n_3, & r > a_2. \end{cases} \tag{26}$$

Here n_1 and n_2 are the unperturbed core index and cladding index, respectively, Λ is the period of the grating, m is the fringe visibility of the index change, and $\overline{\delta n}(z)$ is the "dc" index change spatially averaged over a grating period.

The transverse coupling coefficient between two modes ν and μ is

$$K'_{\nu\mu}(z) = \frac{\omega}{4}\int_0^{2\pi}\mathrm{d}\phi\int_0^{\infty} r\mathrm{d}r\Delta\varepsilon(r,z)\boldsymbol{E}_\nu^{\mathrm{t}}(r,\phi)\cdot\boldsymbol{E}_\mu^{\mathrm{t}*}(r,\phi), \tag{27}$$

where the superscript t denotes transverse vector components only (radial and azimuthal) and the quantity $\Delta\varepsilon(r,z)$ describes the ultraviolet-induced perturbation, here assumed to be independent of ϕ. We neglect the longitudinal coupling coefficients $K_{\nu\mu}^z(z)$ since it is 2–4 orders of magnitude smaller than $K_{\nu\mu}^{\mathrm{t}}(z)$. Assuming the perturbation to be a small fraction of the refractive index, it follows that

$$\Delta\varepsilon(r,z)\approx\begin{cases}2\varepsilon_0 n_1\overline{\delta n}(z)[1+m\cos(2\pi z/\Lambda)], & r\le a_1,\\ 2\varepsilon_0 n_2\overline{\delta n}(z)[1+m\cos(2\pi z/\Lambda)], & a_1<r\le a_{\rm in},\\ 0, & r>a_{\rm in}.\end{cases}\tag{28}$$

Defining the coupling constant $\kappa_{\nu\mu}$ through

$$K^{\rm t}_{\nu\mu}(z)=\kappa_{\nu\mu}(z)[1+m\cos(2\pi z/\Lambda)],\tag{29}$$

we can write the coupling constant for core-mode-core-mode coupling specifically as

$$\begin{aligned}\kappa^{\rm co-co}_{01-01}(z)=&\frac{\omega\varepsilon_0 n_1\overline{\delta n}(z)}{2}\int_0^{2\pi}{\rm d}\phi\int_0^{a_1}r{\rm d}r(|E^{\rm co}_r|^2+|E^{\rm co}_\phi|^2)\\&+\frac{\omega\varepsilon_0 n_2\overline{\delta n}(z)}{2}\int_0^{2\pi}{\rm d}\phi\int_{a_1}^{a_{\rm in}}r{\rm d}r(|E^{\rm co}_r|^2+|E^{\rm co}_\phi|^2).\end{aligned}\tag{30}$$

Using the expressions for fields (1)–(3) and performing the integrals, we obtain

$$\begin{aligned}\kappa^{\rm co-co}_{01-01}(z)=&\overline{\delta n}(z)\frac{2\pi}{\lambda}\frac{2w^2n_1}{V^2n_2}\left[1+\frac{{\rm J}_0^2(u)}{{\rm J}_1^2(u)}\right]+\overline{\delta n}(z)\frac{2\pi}{\lambda}\frac{2u^2}{V^2}\frac{1}{{\rm K}_1^2(w)}\frac{1}{a_1^2}\\&\times\{a_{\rm in}^2[{\rm K}_0^2(wa_{\rm in}/a_1)-{\rm K}_1^2(wa_{\rm in}/a_1)]-a_1^2[{\rm K}_0^2(w)-{\rm K}_1^2(w)]\}.\end{aligned}\tag{31}$$

The coupling constant for core-mode-cladding-mode coupling is

$$\begin{aligned}\kappa^{\rm cl-co}_{1\nu-01}(z)=&\frac{\omega\varepsilon_0 n_1\overline{\delta n}(z)}{2}\int_0^{2\pi}{\rm d}\phi\int_0^{a_1}r{\rm d}r(E^{\rm cl}_rE^{\rm co*}_r+E^{\rm cl}_\phi E^{\rm co*}_\phi)\\&+\frac{\omega\varepsilon_0 n_2\overline{\delta n}(z)}{2}\int_0^{2\pi}{\rm d}\phi\int_{a_1}^{a_{\rm in}}r{\rm d}r(E^{\rm cl}_rE^{\rm co*}_r+E^{\rm cl}_\phi E^{\rm co*}_\phi).\end{aligned}\tag{32}$$

Using Eqs.(1)–(5) and performing the integral in the first term in Eq.(29), we obtain

$$\begin{aligned}\kappa^{\rm cl-co}_{1\nu-01}(z)=&\overline{\delta n}(z)\frac{2\pi}{\lambda}\frac{w}{V}\left(\frac{2\pi}{Z_0n_2}\right)^{1/2}\frac{n_1u_1}{u_1^2-Vu/a_1^2}\left(1+\frac{\sigma_2\xi_0}{n_1^2}\right)E^{\rm cl}_{1\nu}\\&\times\left[u_1{\rm J}_1(u_1a_1)\frac{{\rm J}_0(u)}{{\rm J}_1(u)}-\frac{u}{a_1}{\rm J}_0(u_1a_1)\right]\\&+\frac{\omega\varepsilon_0 n_2\overline{\delta n}(z)}{2}\int_0^{2\pi}{\rm d}\phi\int_{a_1}^{a_{\rm in}}r{\rm d}r(E^{\rm cl}_rE^{\rm co*}_r+E^{\rm cl}_\phi E^{\rm co*}_\phi).\end{aligned}\tag{33}$$

Note that the coupling constants are directly proportional to the "dc" induced-index change $\overline{\delta n}(z)$. The remaining factors in the coupling constant expressions are determined entirely by the dielectric structure of the fibre as shown in Fig.1 and the resulting mode characteristics at a wavelength λ.

To explain why the photosensitive inner cladding can suppress the coupling between the $\rm LP_{01}$ core mode and the $\rm HE^{cl}_{1\nu}$ cladding modes, we calculate the coupling constants of the PS-RMS-50 fibre shown in Fig.1. The fibre is described by the following parameters: core radius a_1=2.5μm, inner cladding radius $a_{\rm in}$=4.9μm, outer cladding radius a_2=62.35μm, numerical aperture is 0.20, the core refractive index is 1.464 at 1550nm, the inner cladding refractive index is the same as the outer, which is 1.444 at 1550nm. The core is doped with germanium, the inner cladding dopants are B_2O_3 and GeO_2, the outer cladding is pure silica.

Figure 2 shows the coupling constant for the core-mode-core-mode coupling in Eq.(31) divided by $\overline{\delta n}(z)$ versus the radius of the photosensitive inner cladding.

Obviously, the coupling constant for core-mode-core-mode coupling increases with the radius of the photosensitive inner cladding. In other words, the grating induced in the photosensitive inner cladding strengthens the coupling between the core mode and itself.

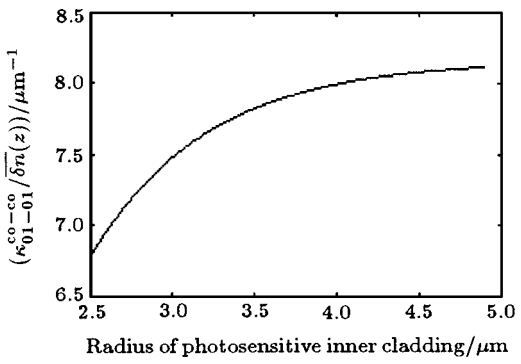


Fig.2. Coupling constant κ_{01-01}^{co-co} divided by $\overline{\delta n}(z)$ versus the radius of photosensitive inner cladding.

Figure 3 shows the coupling constant for the core-mode-cladding-mode coupling in Eq.(33) divided by $\overline{\delta n}(z)$ versus the radius of the photosensitive inner cladding. We show the coupling between three cladding modes ($HE_{1,3}$, $HE_{1,13}$ and $HE_{1,23}$) for example. Opposite to Fig.2, the coupling constant for the coupling of the LP_{01} core mode to the $HE_{1\nu}$ cladding modes decreases with the radius of the photosensitive inner cladding. That is to say, the better suppression effect will be obtained with greater radius of the photosensitive inner cladding. So the grating induced in the photosensitive inner cladding diminishes the coupling interactions between the core mode and the cladding modes.

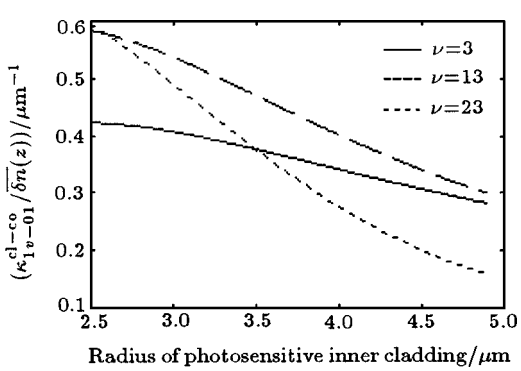


Fig.3. Coupling constant $\kappa_{1\nu-01}^{cl-co}$ divided by $\overline{\delta n}(z)$ versus the radius of photosensitive inner cladding.

In general, the photosensitive inner cladding cannot only suppress the coupling from the LP_{01} core mode to the $HE_{1\nu}^{cl}$ cladding modes but also enhance the coupling of the LP_{01} core mode to itself.

2.3. Coupled-mode equations

The coupled-mode equations that describe counterpropagating interactions in a short-period grating are given by[7]

$$\frac{dA^{co}}{dz} = i\kappa_{01-01}^{co-co}A^{co} + i\frac{m}{2}\kappa_{01-01}^{co-co}B^{co}\exp(-i2\delta_{01-01}^{co-co}z) + i\sum_{\nu}\frac{m}{2}\kappa_{1\nu-01}^{cl-co}B_{\nu}^{cl}\exp(-i2\delta_{1\nu-01}^{cl-co}z), \quad (34)$$

$$\frac{dB^{co}}{dz} = -i\kappa_{01-01}^{co-co}B^{co} - i\frac{m}{2}\kappa_{01-01}^{co-co}A^{co}\exp(+i2\delta_{01-01}^{co-co}z), \quad (35)$$

$$\sum_{\nu}\left[\frac{dB_{\nu}^{cl}}{dz} = -i\frac{m}{2}\kappa_{1\nu-01}^{cl-co}A^{co}\exp(+i2\delta_{1\nu-01}^{cl-co}z)\right], \quad (36)$$

where A^{co} and B^{co} are the amplitudes for the core mode, A_{ν}^{cl} and B_{ν}^{cl} are the amplitudes for the νth cladding mode, and the small-detuning parameters are defined as

$$\delta_{01-01}^{co-co} \equiv \frac{1}{2}\left(2\beta_{01}^{co} - \frac{2\pi}{\Lambda}\right), \quad (37)$$

$$\delta_{1\nu-01}^{cl-co} \equiv \frac{1}{2}\left(\beta_{01}^{co} + \beta_{1\nu}^{cl} - \frac{2\pi}{\Lambda}\right). \quad (38)$$

The approximate centre wavelength of the LP_{01}-LP_{01} Bragg reflection resonant can be found by

$$\delta_{01-01}^{co-co} + \kappa_{01-01}^{co-co} = 0 \quad (39)$$

for the resonance associated with the $HE_{1\nu}$ cladding mode and the LP_{01} core mode is given by

$$\delta_{1\nu-01}^{cl-co} + \kappa_{01-01}^{co-co}/2 = 0. \quad (40)$$

3. Comparison of theory and experiment

In this section we compare experimentally measured transmission spectrum with theoretically calculated transmission spectrum to examine the accuracy of the theory.

Figure 4 shows the measured transmission spectrum through a Bragg grating written in PS-RMS-50 fibre. The optical spectrum analyser used in this experiment is Agilent 86142B. The structure of the cladding mode suppression fibre (PS-RMS-50) is shown in Fig.1. The grating is a uniform Bragg grating with a length of L=8mm, a period of Λ=535.295nm, a visibility of m=0.6 and a "dc" index change of $\overline{\delta n}(z) = \delta n = 2.17 \times 10^{-4}$. It was written

with a CW frequency-doubled argon laser (300C FreD from Coherent). The strong resonance at 1557.65nm is due to LP_{01}-LP_{01} Bragg reflection; the peak reflectivity is –30.6dB. The resonances at shorter wavelengths are caused by coupling to the ν=1,3,5,$\cdots$ cladding modes. Figure 5 shows a theoretical calculation of the transmission through such a grating.

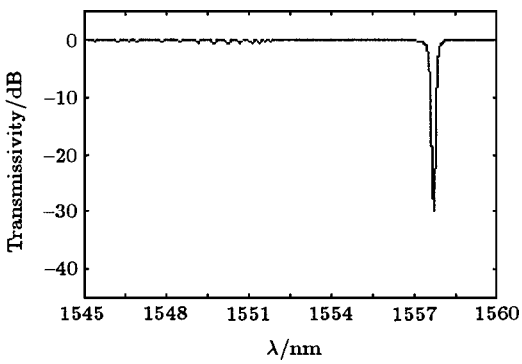


Fig.4. Experimentally measured transmission spectrum through a strong Bragg grating written in a PS-RMS-50 fibre.

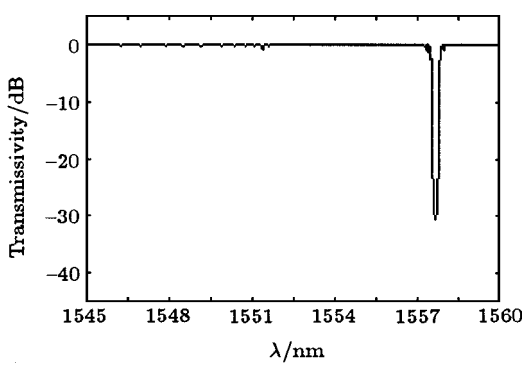


Fig.5. Theoretically calculated transmission spectrum through a strong Bragg grating written in a PS-RMS-50 fibre.

In order to show the suppression effect of the PS-RMS-50 fibre, we have written another grating in a conventional fibre (PS-SMF-30) with a photosensitive core. Figure 6 shows the measured transmission spectrum of it. There is a series of loss peaks with a maximum of 3.5dB at shorter wavelengths.

Compare Fig. 4 with Fig. 6, we see that the maximum loss peak in Fig.6 is up to 3.5dB, whereas in Fig.4 the loss peaks are suppressed to less than 0.5dB. We see that the cladding mode suppression fibre (PS-RMS-50) does show a very obvious suppression effect of the coupling between the core mode and the cladding modes.

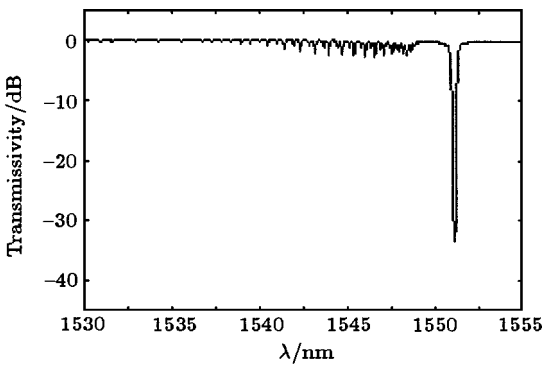


Fig.6. Experimentally measured transmission spectrum through a strong Bragg grating written in a PS-SMF-30 fibre.

Comparing Fig.4 with Fig.5, we find that the loss peaks in Fig.4 are suppressed to less than 0.5dB, but in Fig.5 they are reduced to less than 0.3dB. This is probably because the photosensitivity of the inner cladding is a little weaker than that of the core. Considering this factor, we can say that there is excellent agreement in terms of both the locations and strengths of the resonances.

4. Conclusion

A theory has been presented to analyse the spectral characteristics of optical Bragg gratings written in the cladding mode suppression fibre with a photosensitive inner cladding. The theoretical results indicate that the photosensitive inner cladding cannot only suppress the coupling from the LP_{01} core mode to the $HE_{1\nu}^{cl}$ cladding modes but also enhance the coupling of the LP_{01} core mode to itself. Furthermore, the excellent agreement between the experimental and the theoretical results has testified the accuracy of the theory.

References

[1] Rebola J L and Cartazo A V T 2002 *J. Lightwave Technol.* **20** 1537

[2] Kawanishi T, Oikawa S and Izutsu M 2002 *J. Lightwave Technol.* **20** 1408

[3] Wang M G, Wei H and Jian S S 2003 *Acta Phys. Sin.* **52** 609 (in Chinese)

[4] Xu X H and Cui Y P 2003 *Acta Phys. Sin.* **52** 96 (in Chinese)

[5] Ke H, Peng J H and Fan C C 2001 *IEEE Photon. Technol. Lett.* **13** 1194

[6] Delevaque E *et al* 1995 *Technol. Dig. Conf. Opt. Fibre Commun.* (San Diego CA)

[7] Erdogan T 1997 *J. Opt. Soc. Am.* A **14** 1760